Human Walking Model Predicts Joint Mechanics, Electromyography and Mechanical Economy

Ken Endo, and Hugh Herr, *Member, IEEE*

Abstract— In this paper, we present an under-actuated model of human walking, comprising only a soleus muscle and flexion/extension monoarticular hip muscles. The remaining muscle groups of the human leg are modeled using quasi-passive, series-elastic clutch elements. We hypothesize that series-elastic clutch units spanning the knee joint in a musculoskeletal arrangement can capture the dominant mechanical behaviors of the human knee in level-ground walking. As an evaluation of the musculoskeletal model, we vary model parameters, or spring constants, and muscle control parameters using an optimization scheme that maximizes walking distance and minimizes the mechanical economy of walking. We used a positive force feedback reflex control for the model's soleus muscle, and upper body position control for the hip muscles. The model's clutches were engaged/disengaged using simple state machine controllers. For model evaluation, a forward dynamics simulation was conducted, and the resulting mechanics were compared to human walking data. The model makes qualitative predictions of joint mechanics, electromyography and mechanical economy.

I. INTRODUCTION

In order to design mechanically economical, low-mass leg structures for robotic, exoskeletal and prosthetic systems, designers have often employed passive and quasi-passive components [1-5, 8-11]. In this paper, a quasi-passive device refers to any controllable element that cannot apply a non-conservative, motive force. Quasi-passive devices include, but are not limited to, variable-dampers, clutches, and combinations of variable-dampers/clutches that work in conjunction with other passive components such as springs.

The use of quasi-passive devices in leg prostheses has been the design paradigm for over three decades, resulting in leg systems that are lightweight, energy efficient, and operationally quiet. In the 1970's, Professor Woodie Flowers at MIT conducted research to advance the prosthetic knee joint from a passive, non-adaptive mechanism to an active device with variable-damping capabilities [1]. Using Flowers' knee, the amputee experienced a wide range of knee damping values throughout a single walking step. During ground contact, high knee damping inhibited knee buckling, and swing phase damping allowed for a smooth deceleration of the swinging leg. Motivated by Flowers' research, several research groups developed computer-controlled, variable-damper knee prostheses that ultimately led to

commercial products [2-5]. Actively controlled knee dampers offer clinical advantages over mechanically passive knee designs. Most notably, transfemoral amputees walk across level ground surfaces and descend inclines/stairs with greater ease and stability [6], [7].

Quasi-passive devices have also been employed in the design of economical bipedal walking machines and legged exoskeletons. Passive dynamic walkers [8] have been constructed to show that bipedal locomotion can be energetically economical. In such a device, a human-like pair of legs settles into a natural gait pattern generated by the interaction of gravity and inertia. Although a purely passive walker requires a modest incline to power its movements, researchers have enabled robots to walk across level ground surfaces by adding just a small amount of energy at the hip or the ankle joint [9, 10]. In the area of legged exoskeletal design, passive and quasi-passive elements have been employed to lower exoskeletal weight and to lower system energy usage. In numerical simulation, Bogert [11] showed that an exoskeleton using passive elastic devices can, in principle, substantially reduce muscle force and metabolic energy usage in walking. Walsh et al. [12] built an under-actuated, quasi-passive exoskeleton designed for load-carrying augmentation. During level-ground walking, the exoskeleton only required 2 Watts of electrical power for its operation with on average 80% load transmission through the robotic legs.

Although passive and quasi-passive devices have been exploited to improve overall system economy in legged systems, the resulting structures failed to truly mimic human-like joint mechanics in level-ground ambulation. In this paper, we seek to understand how leg muscles and tendons work mechanically during walking in order to motivate the design of economical, low-mass robotic legs. We present an under-actuated model of human walking, comprising only a soleus muscle and flexion/extension monoarticular hip muscles. The remaining muscle groups of the human leg are modeled using quasi-passive, series-elastic clutch elements spanning the model's hip, knee and ankle joints in a musculoskeletal arrangement. We hypothesize that the series-elastic clutch units spanning the model's knee joint can capture the dominant mechanical behaviors of the human knee in level-ground walking. Since the human knee performs net negative work throughout a level-ground walking cycle [13], and since a series-elastic clutch is incapable of dissipating mechanical energy as heat, a corollary to this hypothesis is that such a quasi-passive robotic knee would necessarily have to transfer energy via elastic biarticular mechanisms to hip and/or ankle joints.

Ken Endo is with Biomechatronics group, Media lab, Massachusetts Institute of Technology, Cambridge, MA 02139 USA (phone: 617-253-2941; fax: 617-253-8542; e-mail: kene@media.mit.edu).

Hugh Herr is with Biomechatronics group, Media lab, Massachusetts Institute of Technology, Cambridge, MA 02139 USA (e-mail: hherr@media.mit.edu).
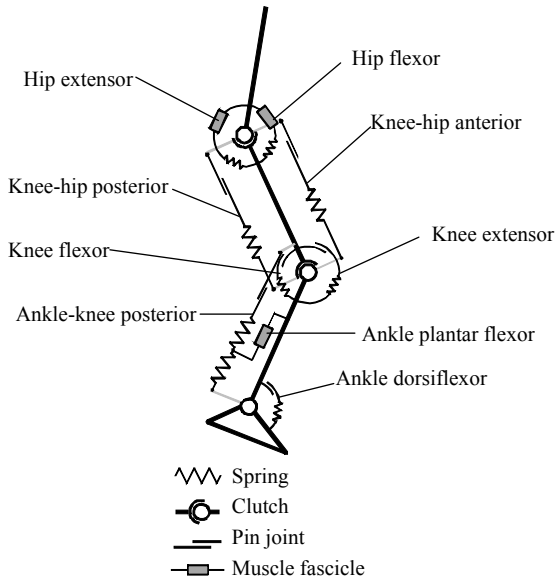
Fig. 1. Three-muscle leg model. Only three muscles act about the model's ankle and hip joints. Series-elastic clutch units span the model's ankle, knee and hip in a musculoskeletal arrangement.

Such a transfer of energy would reduce the necessary actuator work at the hip and ankle, improving the mechanical economy of a human-like walking robot. For model evaluation, a forward dynamics simulation is adopted and the resulting mechanics are compared to human walking data. We vary model parameters, or spring constants, and muscle control parameters using an optimization scheme that maximizes walking distance and minimizes the mechanical economy of walking. Forward dynamics simulation is required to evaluate both morphology and controller. We use a positive force feedback reflex control for the model's soleus muscle, and upper body position control for the hip monoarticular muscles. Finally, the model's clutches are engaged/disengaged using simple state machine controllers.

II. METHODOLOGY

A. Musculoskeletal Model

1) Leg Architecture

Fig. 1 shows a two-dimensional musculoskeletal model of the human leg comprising nine series-elastic clutch/muscle mechanisms. The model was derived by inspection of the human musculoskeletal architecture. For isometric and eccentric contractions, metabolic load is relatively less than concentric contractions. We hypothesized that humans walk economy by actuating muscles that span the knee joint isometrically, with mechanical energy transfer to the hip and ankle to reduce muscle concentric work at those joints. Our previous study [14] revealed that, for a self-selected walking speed, monoarticular hip and ankle muscles are required to capture the dominant mechanics at those joints, but only quasi-passive elements are necessary to capture knee joint mechanics. Similar to this earlier model, the hip monoarticular, extensor/flexor units and the ankle monoarticular, plantar flexor unit are the only active model components shown in Fig. 1 capable of producing net work.

The remaining muscle-tendon units are modeled as series-elastic clutches. For each of these quasi-passive units, when a clutch is disengaged, joints rotate without any resistance from the series spring. Once a clutch is engaged, the series spring is held at its current position, and the spring begins to store energy as the joint rotates, in a manner comparable to a muscle-tendon unit where the muscle generates force isometrically. The model comprises five monoarticular and three biarticular tendon-like springs with series clutches or muscle actuators. It is noted that the ankle-knee posterior unit and the ankle plantar flexor both share the same distal tendon spring (See Fig. 1). Hip, knee and ankle joints have agonist/antagonist pairs of monoarticular springs with series clutches or muscle actuators. Further, the leg model includes two knee-hip and one ankle-knee biarticular units. The knee-hip anterior unit works as an extensor at the knee joint and as a flexor at the hip, while the knee-hip posterior unit works as a flexor at the knee joint and as an extensor at the hip. We assume that all monoarticular units are rotational springs and clutches, while all biarticular units act around attached pulleys with fixed moment arm lengths. The moment arms for biarticular units are taken from the literature [15], [16].

The seven segments of this under-actuated model, namely two feet, two shanks, two thighs and one head-arm-torso (HAT) segment are simple rigid bodies whose mass parameters are estimated from a human study participant (27yr, 1.87m height, 81.9kg weight) [17]. The clutches and muscles are considered massless.

2) Muscle Model

The two hip muscles are in series with linear springs. The ankle plantar flexor is also connected in series with a linear spring, but that spring also attaches to a second spring that spans the knee joint via a clutch mechanism (See Fig. 1). Besides series elasticity (SE), the muscles are modeled as a set of a parallel elasticity (PE), buffer elasticity (BE) and contractile element (CE) in a Hill-type muscle tendon unit (MTU) [18]. The force of the CE is a product of muscle activation A, CE force-length relationship $f_l(l_{CE}, l_{opt})$, and CE force-velocity relationship $f_v(v_{CE})$, or

$$F_{CE} = A F_{max} f_l(l_{CE}, l_{opt}) f_v(v_{CE}) \tag{1}$$

where F_{max} is the maximum isometric force, l_{CE} is the length of the CE, l_{opt} is the optimal length of the CE and v_{ce} is the CE velocity. Based on this product approach, we compute the muscle fascicle dynamics by integrating the CE velocity. A muscle activation A relates to a neutral input S with a first order differential equation describing the excitation-contraction coupling

$$\tau dA(t)/dt = S - A(t) \tag{2}$$

where τ is a time constant. The maximum isometric force and optimal length of ankle plantar flexor muscle, $F_{max,ap}$ and $l_{opt,ap}$, are parameters for the optimization while the

(a) Ankle state machine
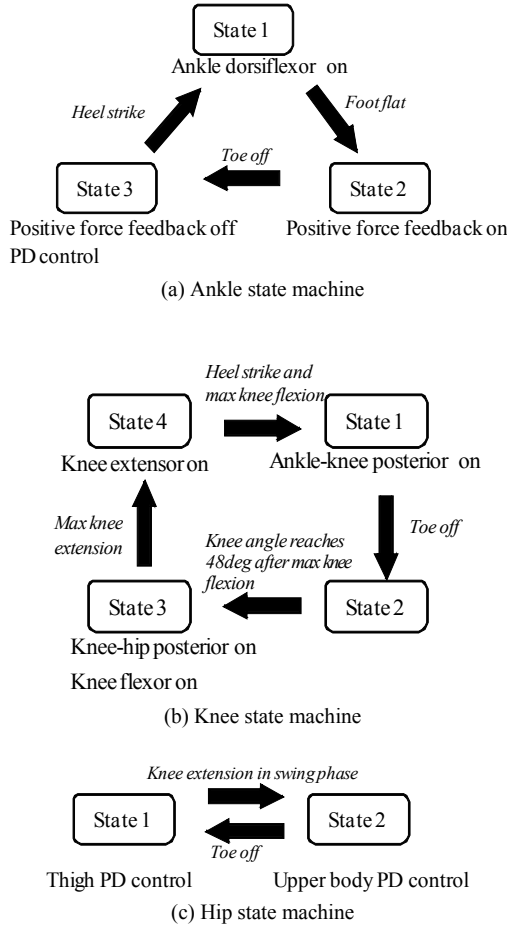
(b) Knee state machine

(c) Hip state machine

Fig. 2. State machine controller for the (a) ankle, (b) knee and (c) hip joints. State transitions are facilitated by the walking model behavior shown in italic text. Each state machine depicts clutch engagement times. A clutch is disengaged automatically when its series spring returns to its equilibrium position after a storage-release cycle.

remaining values are chosen from the literature [18].

B. Controller

The clutches and muscles are controlled based on state machines. The state transitions are facilitated by the human model and its interaction with the walking surface, and each clutch is engaged or muscle activated according to the state. The state machines were constructed such that clutch engagements were triggered by gait events suggested by our previous optimization results [14]. In the next section, we propose two feedback reflex controllers for the three muscles. We also describe in detail the state machines employed in the control of the clutch units.

1) Positive Force Feedback Controller for the Ankle Plantar Flexor

During the stance phase, the soleus muscle generates a large amount of force to plantar flex the ankle. In order to replicate this behavior, positive force feedback is adopted for the ankle plantar flexor control. Under positive force feedback, the stimulation of the ankle planter flexor $S_{ap}(t)$ is calculated as follows:

$$S_{ap}(t) = S_{0,ap} + G_{ap}F_{ap}(t - \Delta t_{ap}) \qquad (3)$$

where $S_{0,ap}$ is a pre-stimulation, G_{ap} is a gain, F_{ap} is the measured muscle force, and Δt_{ap} is a time-delay. The positive force feedback control is turned on only after foot flat (FF) during the stance phase, and is turned off at the time of toe off (TO). During the swing phase, the ankle joint is controlled with a simple proportional-derivative (PD) control with low gain to keep the ankle angle equal to $\theta_{ref,a}$ in preparation for heel strike (HS). The ankle state machine is shown in the following section. In the positive force feedback control, G_{ap} and $\theta_{ref,a}$ are parameters for the optimization, with the remaining parameters taken from the literature [19].

2) Position Controller for the Hip Flexor/Extensor

As the hip flexor and extensor are attached to the HAT segment directly, these two muscles are controlled to balance the HAT during the stance phase. The hip flexor and extensor are stimulated with a PD signal of the HAT's pitch angle θ_H with respect to gravity as follows

$$S_{hip\_flexor/extensor} =$$
$$\pm[k_{p,H}\{\theta_H(t - \Delta t_H) - \theta_{H,ref}\} + k_{d,H}\dot{\theta}_H(t - \Delta t_H)] \qquad (4)$$

where $k_{p,H}$ and $k_{d,H}$ are the proportional and derivative gains, $\theta_{H,ref}$ is a reference lean angle, and Δt_H is a time-delay.

During the swing phase, the swing leg needs to be carried forward in preparation for HS. The hip joint is controlled such that the thigh pitch angle reaches a reference angle as follows:

$$S_{hip\_flexor/extensor} =$$
$$\pm[k_{p,t}\{\theta_t(t - \Delta t_t) - \theta_{t,ref}\} + k_{d,t}\dot{\theta}_t(t - \Delta t_t)] \qquad (5)$$

where $k_{p,t}$ and $k_{d,t}$ are the proportional and derivative gains, $\theta_{t,ref}$ is a reference thigh angle in the global axis, and Δt_t is a time-delay. In the hip position controller, $k_{p,H}$, $k_{d,H}$, $\theta_{H,ref}$, $k_{p,t}$, $k_{d,t}$ and $\theta_{t,ref}$ are parameters for the optimization, and the remaining values are taken from the literature [19].

3) State Machine

Fig. 2 shows state machines for controlling (a) the ankle, (b) knee and (c) hip joints. The state machines turn on/off the muscle controller and engage the clutches, while each clutch is disengaged automatically, when its series spring returns to its equilibrium point.

The ankle state machine is composed of three states. Starting in State 3, State 1 begins at HS. In State 1, the clutch in the ankle dorsiflexor is engaged. The controller transitions from State 1 to State 2 at the time of FF, at which time the positive force feedback control is initiated. The controller transitions from State 2 to State 3 at toe off (TO). In State 3, the positive force feedback is turned off, and the low-gain PD controller is applied at the ankle joint in order to keep the ankle angle equal to $\theta_{a,ref}$ in preparation for HS. At the next HS, the controller transitions from State 3 to State 1 again.

For the knee state machine controller, there are four states. From State 4, the controller transitions to State 1 at maximum knee flexion during the stance phase following HS. In State 1, the ankle-knee posterior clutch is engaged. The transition from State 1 to State 2 is triggered by TO. Then, the knee-hip anterior is engaged. In State 2, the controller transitions from State 2 to State 3, when the knee angle reaches 48deg after maximum flexion during the swing phase. The knee-hip

posterior and knee flexor are engaged in State 3. Finally, the controller goes back to State 4 from State 3, when the knee joint reaches maximum extension in the swing phase. The knee extensor is engaged in State 4.

The hip state machine controller includes only two states. In State 1, the hip controller transitions from State 1 to State 2 at the maximum knee extension in the swing phase, and from State 2 to State 1 at TO. The hip muscles are controlled with the thigh and HAT PD control in State 1 and State 2, respectively.

C. Optimization

The model has a total of 19 parameters: nine spring constants and 10 Hill-type muscle control parameter: $F_{max,ap}$, $l_{opt,ap}$, G_{ap}, $\theta_{ref,a}$, $k_{p,H}$, $k_{d,H}$, $\theta_{H,ref}$, $k_{p,t}$, $k_{d,t}$ and $\theta_{t,ref}$. Parameters were evaluated with a walking forward dynamics simulation. The cost function was defined as follows:

$$\cos t = \begin{cases} 10/(D+N) & \text{if the model falls down within 10} \quad (6) \\ & \text{walking gait cycles} \\ c_{mt} & \text{otherwise} \quad (7) \end{cases}$$

where D is the walking distance, N is the number of steps, and c_{mt} is the mechanical economy. Mechanical economy was defined as

$$c_{mt} = W^+/(MD) \quad (8)$$

where W^+ is the total positive mechanical work done by the three muscles and M is body weight [10].

The determination of the desired global minimum for this objective function was implemented by first using a genetic algorithm to find the region containing the global minimum, followed by the use of an unconstrained gradient optimizer (fminunc in Matlab) to determine the exact value of that global minimum.

The optimizer found parameters that enabled the model to walk more than 10 walking gait cycles without falling down using cost function (6). If the musculoskeletal model was capable of walking more than 10 walking gait cycles, cost function (7) was then employed. Cost function (7) was always less than cost function (6) so that the optimizer selected parameters that enabled both robust and economical walking [20, 21].

D. Forward Dynamics Simulation

A MATLAB SIMULINK model of the system was developed based on the musculoskeletal model. The Simulink model was simulated using the stiff/NDF algorithm (ode15s routine built in MATLAB).

The forward dynamics simulation started with the right foot HS. Initial angle and angular velocity of each joint were taken from a human study participant (27yr, 1.87m height, 81.9kg weight). We also applied the same initial walking velocity at the center of mass (COM).

Each foot segment of the bipedal model has contact points at its toe and heel. When impacting the ground, a contact point gets pushed back by a vertical reaction force F_y:

$$F_y = -k_v g_l(\Delta y) g_v(\Delta \dot{y}) \quad (8)$$

TABLE I
SIMULATION RESULTS

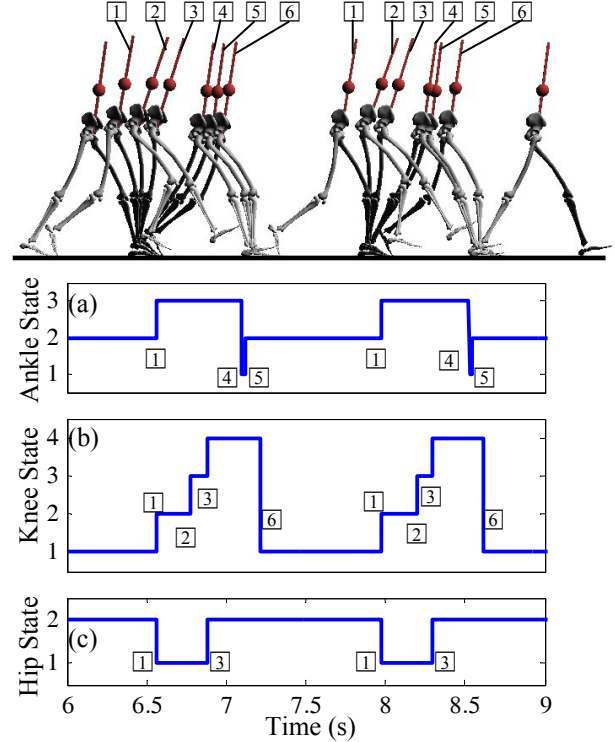|	Musculoskeletal Model	Human
walking Speed (m/s)	1.20	1.27
stride time (s)	1.43	1.22
step length (m)	0.85	0.77
mechanical economy	0.044	0.055

Fig. 3 Finite-state control transitions of the (a) ankle, (b) knee, and (c) hip joints during steady state walking (from t=6s to 9s). The controllers transitions from states to states according the events: ① toe off, ② knee angle reaches 48 deg after maximum knee flexion during the swing phase, ③ maximum knee extension, ④ heel strike ⑤ foot flat, and ⑥ maximum knee flexion. As the heel strike and foot flat happens almost at the same time, the ankle state machine controller transitions rapidly from State 3 to State 2.

Where k_v is a spring coefficient, Δy is vertical penetration length, g_l is a force-length relationship, and g_v is a force-velocity relationship. A horizontal reaction force is modeled as a kinetic friction force that opposes the CP's motion on the ground with a force F_x:

$$F_x = u_{sl} F_y \quad (9)$$

where u_{sl} is a kinetic friction coefficient. When the CP slows down to below a speed v_{lim}, we model the horizontal reaction force as a stiction force computed in a similar way to equation (8) [22].

III. RESULT

In this section, we present the results obtained from the optimization. The model's walking speed, stride time, step length and mechanical economy are shown in TABLE I along with values from a weight and height-matched walking
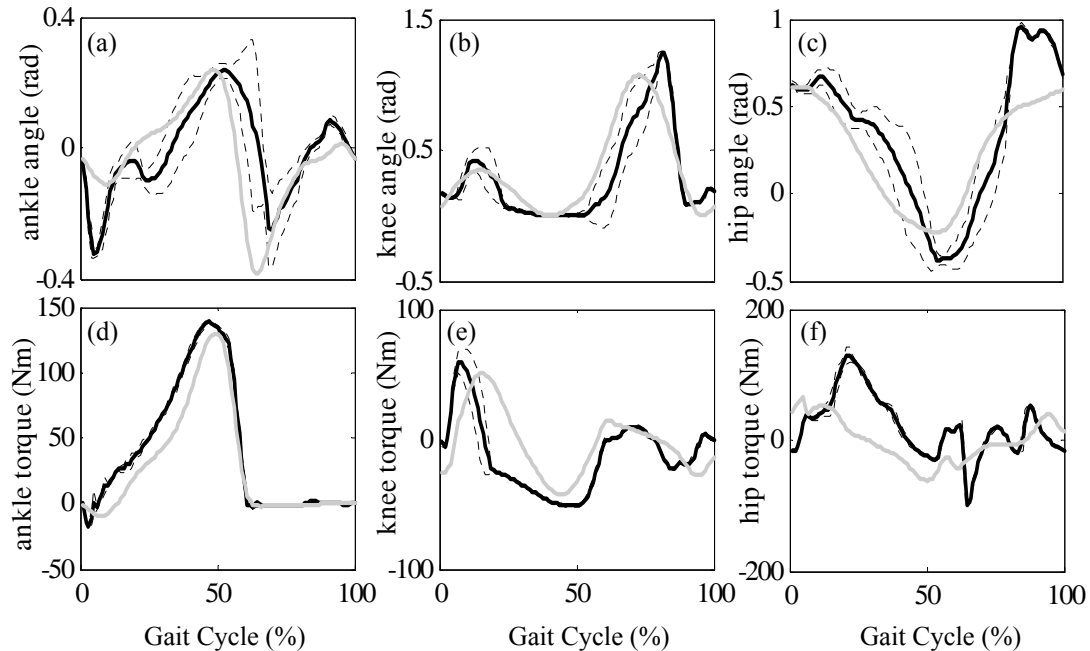
Fig. 4 Angle and torque of the leg model in the forward dynamics simulation: (a) ankle angle, (b) knee angle, (c) hip angle, (d) ankle torque, (e) knee torque, and (f) hip torque. Black and grey solid curves are simulation results and biological data, respectively. Each dotted curve is one standard deviation from the black solid curve. Each curve starts from the heel strike and ends with the heel strike of the same leg. These are average data of 10 steps in the steady state walking.

human. Though walking speed is a bit slower, and stride time and step length are longer, the musculoskeletal model walks with lower mechanical economy than the human walker.

The model's state machines performed properly throughout the walking cycle. Fig. 3 shows data for two consecutive walking cycles during steady state walking (from 6 seconds to 9 seconds in the forward dynamics simulation). The controller transitions from state to state facilitated by gait events: ① TO, ② knee angle reaches 48deg after maximum flexion during the swing phase, ③ maximum knee extension, ④ HS ⑤ FF, ⑥ maximum knee flexion during the stance phase. The control system sequenced though this pattern during each walking cycle.

In Fig. 4, (a) the ankle angle, (b) the knee angle, (c) the hip angle, (d) the ankle torque, (e) the knee torque, and (f) the hip torque are plotted versus percent gait cycle. Each curve begins at HS and ends with the HS of the same leg. Black and grey curves are simulation results and biological data from a weight and height-matched walking person, respectively. Dotted curves are one standard deviation from the mean. These data are the averages of 10 steps in steady state walking. The model makes qualitative predictions of ankle, knee and hip mechanics.

Fig. 5 shows the torque or force contribution of each muscle or clutch. The thick horizontal lines indicate the activation periods of the corresponding muscle electromyography (EMG) [23]. The model's clutch engagement and muscle activation times qualitatively matched the EMG signals, with the exception of the hip extensor.

IV. DISCUSSION

The walking simulation had a lower mechanical economy than the weight and height-matched walking human. Perhaps the model's mechanical economy was lower because the value was calculated from only the positive mechanical work done by the three muscle actuators in each leg of the model. Positive work contributions from the upper body and contributions from walking in three dimensions were not included in the model, and perhaps might explain the observed difference in economy.

The walking model makes qualitative predictions of joint mechanics, electromyography and mechanical economy. The poorest agreement between model and human data were at the hip. We believe this lack of predictive power was the consequence of using a simple PD controller at this joint. With the hip state machine, the HAT PD controller and thigh PD controller were switched by HS and TO. This transition generated 1) large positive torque only after HS and 2) large negative torque after TO, while in contrast the human generated large positive torque during the swing phase, and large negative torque during the stance phase. The hip angle also exceeded the biological hip angle at the terminal swing phase. In future work, we therefore wish to develop a more biologically realistic controller for the hip extensor and flexor muscles.

V. CONCLUSION

We presented an under-actuated model of human walking, comprising only a soleus muscle and flexion/extension monoarticular hip muscles. The remaining muscle groups of
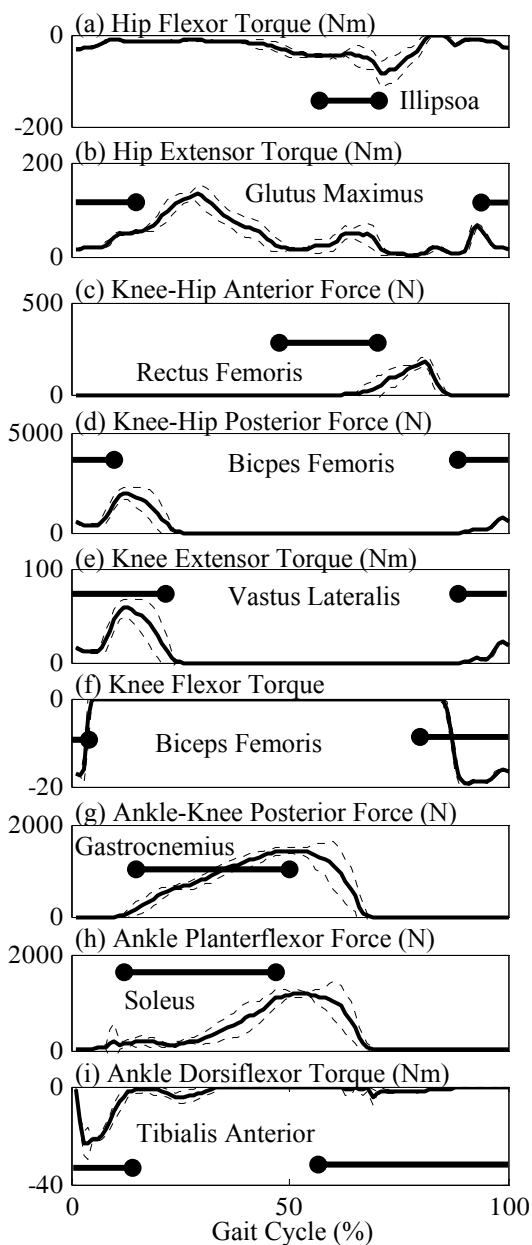
Fig. 5 Torque and Force generated from (a) hip flexor, (b) hip extensor, (c) knee-hip anterior, (d) knee-hip posterior, (e) knee extensor, (f) knee flexor, (g) ankle-knee posterior, (h) ankle planterflexor and (i) ankle dorsiflexor. Black solid and dotted curves are torque or force, and one standard deviation from the solid line. Corresponding muscle EMGs are shown as horizontal solid lines with two circles at the edges.

the human leg were modeled using quasi-passive, series-elastic clutch elements. As an evaluation of our hypotheses, the model parameters, or spring constants, and muscle control parameters were optimized such that resulting walking economy was minimized. As muscle controllers, a positive force feedback reflex control for the model's soleus muscle, and upper body position control for the hip muscles were employed. The model's clutches were engaged/disengaged using simple state machine controllers. The model made qualitative predictions of joint mechanics, electromyography and mechanical economy. In the development of low-mass, highly economical prostheses, orthoses, exoskeletons, and humanoid robots, we feel elastic

energy storage and human-like leg musculoskeletal architectures are design features of critical importance.

REFERENCES

[1] W. C. Flowers, "A Man-Interactive Simulator System for Above-Knee Prosthetics Studies,", Ph.D. thesis, Department of Mechanical Engineering, MIT, Cambridge, MA, 1972.

[2] K. James, R.B. Stein, R. Rolf, D. Tepavic, "Active suspension above-knee prosthesis, " in *1990 Proc. of the 6th Int. Conf. on Biomedical Engineering*, p.346.

[3] I. Kitayama, N. Nakagawa, K. Amemori, "A microcomputer controlled intelligent A/K prosthesis," in *1992 Proc. of the 7th World Congress of the International Society for Prosthetics and Orthotics*.

[4] S. Zahedi, "The results of the field trial of the Endolite Intelligent Prosthesis," in *1993 XII Int. Cong. of INTERBOR*.

[5] H. Herr, A. Wilkenfeld, "User-adaptive control of a magnetorheological prosthetic knee, " *Industrial Robot: An International Journal*. vol. 30, pp.42–55, 2003.

[6] L. J. Marks, J. W. Michael, "Science, medicine, and the future. Artificial limbs," *BMJ*, vol. 323, pp. 732-735, 2001.

[7] J. Johansson, D. Sherrill, P. Riley P, P. Paolo B, H. Herr, "A Clinical Comparison of Variable-Damping and Mechanically-Passive Prosthetic Knee Devices," *American Journal of Physical Medicine & Rehabilitation, vol.* 84(8), pp.563-575, 2005.

[8] T. McGeer, "Passive Dynamic Walking," *International Journal of robotics research*, vol. 9, no. 2, pp62-82, 1990.

[9] M. Wisse, "Essentials of Dynamic Walking, Analysis and Design of two-legged robots," PhD Thesis, Technical University of Delft, 2004.

[10] S. Collins, and A. Ruina, "A Bipedal Walking Robot with Efficient and Human-Like Gait", in *2005 Proc. Int. Conf. Robotics and Automation*, pp.1983-1988.

[11] A. J van den Bogert, "Exotendons for assistance of human locomotion," B*iomedical Engineering Online*, vol. 2, 2003.

[12] C. J. Walsh, K. Endo, and H. Herr, "Quasi-passive leg exoskeleton for load-carrying augmentation," *Int. J. Hum. Robot.* vol. 4, no. 3, pp. 487–506, 2007.

[13] D. Winter, "Biomechanics and Motor Control of Human Movement,"New York: John Wiley & Sons, 1990.

[14] K. Endo, and H. Herr, "A model of Muscle-Tendon Function in Human Walking,", in *2009 Proc of IEEE International Conference on Robotics and Automation (ICRA), 2009*.

[15] M. Gunther, and H. Ruder, "Synthesis of two-dimentional human walking: a test of the lambda-model," Bio. Cybern.,vol. 89, pp89-106, 2003.

[16] M.P. Kadaba, H.K. Ramakrishnan, and M.E. Wootten, "Measurement of lower extremity kinematics during level walking," *J. Orthop. Res.*, vol 8(3), pp.383-392, 1990.

[17] H. Herr, M. Popovic, "Angular Momentum in Human Walking", Journal of Experimental Biology 211, pp.467-48, 2008.

[18] G. T.. Yamaguchi, A.G.U Sawa, D. Moran, M.J. Fessler, J.M. Winter, "A survey of human musculotendon actuator parameter", Multiple Muscle Systems: Biomechanics and Movement Organization. Springer-Verlag, pp.717-778, 1990.

[19] H. Geyer, A. Seyfarth, R. Blickhan, "Positive force feedback in bouncing gaits?," Proceedings of the Royal Society of London, Series B: Biological Science, vol.270(1529), pp.2173-2183, 2003.

[20] H. Naito, T. Inoue, K. Hase, T. Matsumoto, and M. Tanaka, "Development of hip disarticulation prostheses using a simulator based on neuro-musculo-skeletal human walking model,", J. Biomechanics –Abstract of the 5th World Congress of Biomechanics-, Vol.39, Supplement 1, S43(4228), 2006.

[21] K. Hase and N. Yamazaki, "Computer simulation study of human locomotion with a three-dimensional entire-body neuro-musculo-skeletal model, I. Acuisition of normal walking," JSME Int. J., Series C, 45(4), pp.1040-1050, 2002.

[22] K. Gerritsen, A. van den Bogart, B. Nigg, "Direct dynamics simulation of the impact phase in heel-toe running," *J. Biomech.*, vol.28(6), pp.607-627, 2006.

[23] R.L. Lieber, *Skeletal Muscle Structure and Function*, Williams & Wilkins, 1992.